DOI: 10.1002/anie.200701847

Heterometallic Complexes

Long-Range Magnetic Ordering in a Tb^{III}–Mo^{V} Cyanido-Bridged Quasi-One-Dimensional Complex**

Ferry Prins, Edoardo Pasca, L. Jos de Jongh, Huub Kooijman, Anthony L. Spek, and Stefania Tanase**

The search for new supramolecular assemblies exhibiting long-range magnetic ordering has attracted much attention in the last decade.[1–3] In this regard, cyanido-bridged heterobimetallic assemblies derived from $[M(CN)_6]^{3-}$ (M = Cr, Fe, Co) building blocks and various transition metal or rare earth metal ions have been extensively explored.[4–8] More recently, $[M(CN)_8]^{3-/4-}$ (M = Mo, W) anions have become attractive building blocks for the synthesis of new cyanido-bridged networks with remarkable magnetic and photomagnetic properties.[9–11] Octacyanidometallates profit from the enhanced π backbonding and superexchange efficiency resulting from the greater diffuseness and radial distribution of 4d/5d orbitals as compared with 3d orbitals. Therefore, the combination of the anionic octacyanidometallate building blocks with rare earth metal ions that have strong spin–orbit coupling is a challenging route towards new supramolecular magnetic materials with intrinsic anisotropy. The development of such materials has been somewhat hampered by the tendency of the rare earth metal ions to adopt high coordination numbers and their ability to easily adapt to a given environment.[7,12–15] In search of new synthetic methods for d–f cyanido-bridged assemblies from $[M(CN)_8]^{3-/4-}$ (M = Mo, W) building blocks, we rationalized that the N,O-bidentate chelate binding of pyrazine-2-carboxamide (pzam) combined with the ability of NH_2 groups to act as effective electron acceptors towards oxygen to form hydrogen-bonding networks may help in the construction of extended structures and may enhance and improve their bulk magnetic properties. This communication details the synthesis, characterization, and magnetic properties of the first one-dimensional derivative of $[Mo(CN)_8]^{3-}$ and Tb^{III}, namely, $[Tb(pzam)_3(H_2O)Mo(CN)_8]\cdot H_2O$ (**1**).

The reaction of $Tb(NO_3)\cdot 5H_2O$ with $(Bu_3NH)_3[Mo(CN)_8]\cdot 4H_2O$ in the presence of pzam as a small blocking ligand readily affords **1** as a yellow precipitate. After filtration, slow evaporation of the solution yielded single crystals suitable for X-ray analysis, which revealed that **1** is a one-dimensional chain polymer (Figure 1). The coordination sphere around Tb^{III} comprises three pzam ligands with a N,O-bidentate chelate binding, a water molecule, and two cyanido bridges. The nine-coordinate Tb^{III} ion lies in a monocapped square-antiprism environment; N31 is in the capping position, the top plane is formed by O1/N51/O38/N41 and the bottom plane by O18/N11/O28/N21 (Figure 1). The angle between top (capped) and bottom planes is 2.59(15)°. For the top plane the square angles lie in the range 83.69(14)–94.10(15)°, and those of the lower plane are in the range 77.57(16)–102.37(18)°. The geometry of the $[Mo(CN)_8]^{3-}$ unit is approximately square-antiprismatic, with Mo–C bond lengths ranging from 2.139(6) to 2.187(6) Å. The twist angles (top atom–top centroid–bottom centroid–bottom atom) of the Mo^{V} center are in the range 42.6(3)–49.0(3)°. The Mo-C-N angles are almost linear and range from 174.7(6) to 178.4(6)°; however, the cyanido linkages deviate from linearity (Tb1-N41-C41 164.0(5), Tb1-N51-C51 160.8(5)°). The intrachain distances between Tb^{III} and Mo^{V} are 5.6860(10) and 5.7144(10), respectively. The intrachain $Mo^{V}\cdots Mo^{V}$ distance is 10.7845(10) Å.

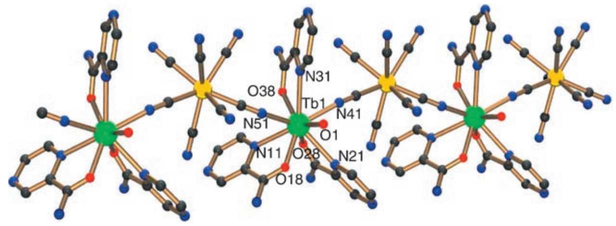

Figure 1. View of the structure of **1** along the *b* axis, showing the one-dimensional chain. Hydrogen atoms omitted for clarity. Tb green, Mo yellow, C black, N blue, O red.

Each Tb^{III}–Mo^{V} chain interacts with six other surrounding chains to form a three-dimensional network structure (Figure 2). Four out of six terminal cyanido ligands of the

---

[*] Dr. E. Pasca, Prof. L. J. de Jongh
Kamerlingh Onnes Laboratory
Leiden Institute of Physics
Leiden University
PO Box 9504, 2300 RA, Leiden (The Netherlands)
Fax: (+31) 71-527-5404
E-mail: jongh@physics.leidenuniv.nl
F. Prins, Dr. S. Tanase
Leiden Institute of Chemistry
Gorlaeus Laboratories
Leiden University
PO Box 9502, 2300 RA, Leiden (The Netherlands)
Fax: (+31) 71-527-4451
E-mail: s.grecea@chem.leidenuniv.nl
Homepage: http://www.chem.leidenuniv.nl/cbac
Dr. H. Kooijman, Prof. A. L. Spek
Bijvoet Center for Biomolecular Research
Crystal and Structural Chemistry
Utrecht University
Padualaan 8, 3584 CH Utrecht (The Netherlands)

[**] The authors acknowledge Prof. Jan Reedijk (Leiden University) for valuable discussions. This research was supported by a Veni grant from the Netherlands Organization for Scientific Research (NWO) to S.T. and the ECNetwork of Excellence Magmanet (No. 515767-2).

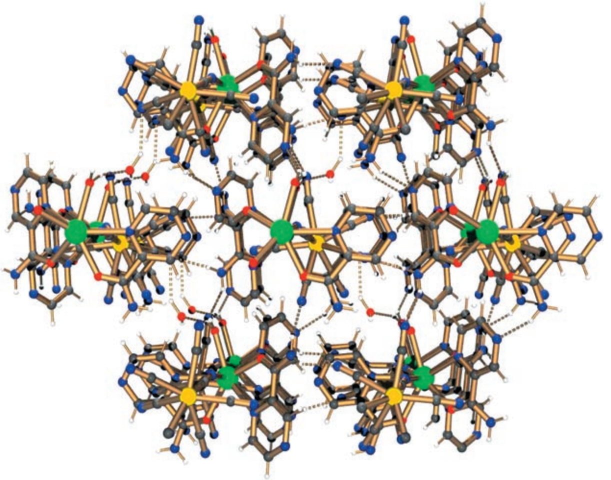

Figure 2. View along the *b* axis of the hydrogen-bonding interactions in **1**. Color code as in Figure 1.

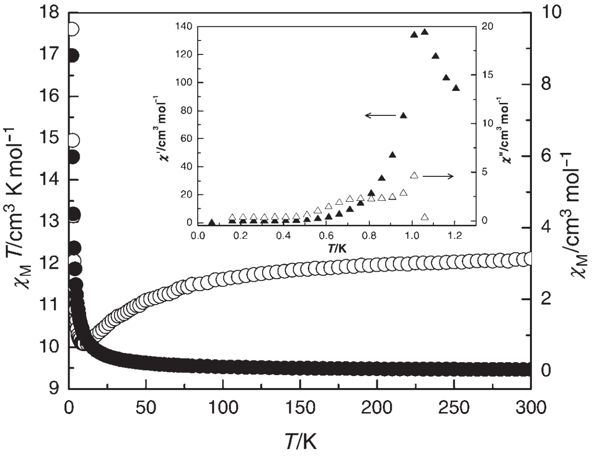

Figure 3. Temperature dependence of $\chi_M T$ (○) and χ_M (●) for **1** measured at 0.1 T. Inset: Temperature dependence of the real (χ_{ac}') and imaginary (χ_{ac}'') components of the ac magnetic susceptibility measured in an applied field of 0 T and at a frequency of 971 Hz.

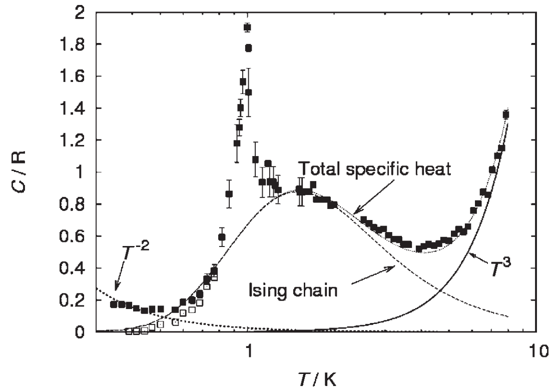

Figure 4. Molar specific heat of **1** as a function of temperature. A sharp peak is visible at $T_c = 1.0$ K. Solid lines represent the contributions from the phonons (T^3), the prediction of the Ising chain with $J = 3.6$ K and two spins $S = 1/2$ per unit cell, and the contribution from the hyperfine-split nuclear levels of Tb^{III} (T^{-2}). Open symbols represent experimental data with hyperfine contribution subtracted.[23]

Mo^V center are involved in hydrogen bonding. Three of them bind interchain to the amide nitrogen atoms of two different ligands of the same chain (N29–H29a···N61 3.310(7), N29–H29b···N64 2.974(7), N19–H19b···N66 2.842(7) Å). One of the two has an additional bond to the noncoordinated water molecule (O2–H2a···N64 3.022(7) Å). The third terminal cyanido ligand of the primary chain interacts with an amide nitrogen atom of a second chain (N19–H19b···N63 2.856(8) Å). This same chain interacts at two more positions. The first involves an amide nitrogen atom of a pzam ligand and a 4-pyrazine nitrogen atom of a pzam ligand (N39–H39a···N24 2.977(6) Å); the second involves the 4-pyrazine nitrogen atom of a pzam ligand and a coordinated water molecule on the other chain (O1–H1b···N14 2.869(6) Å). An additional hydrogen bond is formed between the coordinated and noncoordinated water molecules (O1–H1a···O2 = 2.755(6) Å). The one-dimensional chains run parallel to the *b* axis. In the *a* direction adjacent chains are about 8.053 Å apart, while in the *c* direction the interchain distance is 10.218 Å. The shortest interchain Mo^V···Mo^V distance is 9.709 Å.

The temperature-dependent magnetic susceptibility data for powder samples of **1** (1.8–300 K) are shown in Figure 3 as plots of $\chi_M T$ versus T and χ_M versus T. The observed $\chi_M T$ value at 300 K of 12.1 cm^3 K mol^{-1} corresponds exactly to that calculated for noninteracting Tb^{III} and Mo^V ions (11.75 cm^3 K mol^{-1} for 4f^8 and 0.37 cm^3 K mol^{-1} for 4d^1).[2,16] From 300 to 9 K, the $\chi_M T$ value decreases slightly to 10.09 cm^3 K mol^{-1} and then increases to about 17.6 cm^3 K mol^{-1} at 1.8 K. The initial decrease is attributed to depopulation of the Stark levels of the Tb^{III} $^7F_6$ ground state. Additional ac susceptibility data, recorded down to 0.2 K, display a high and sharp peak at $T_c = 1.0$ K in the real component (χ'_{ac}) that indicates the onset of magnetic ordering (Figure 3). At the same temperature, a sharp peak is also found in the specific heat of **1**, as shown in Figure 4. Below T_c, χ'_{ac} drops to essentially zero. The small bump in the imaginary part χ''_{ac} at and below T_c indicates some magnetic losses in the ordered region. Magnetization data up to 5 T at a number of temperatures are shown in Figure 5.

As discussed below, the observed magnetic behavior of **1** can be consistently explained in terms of ferromagnetic Tb^{III}–Mo^V chains, coupled by weak interchain interactions of mainly dipolar origin, that lead to a transition to 3D long-range magnetic ordering between the chains at $T_c = 1.0$ K. For the Mo^V magnetic moment we can assume a spin of $S = 1/2$ with an isotropic g factor; for the Tb^{III} magnetic moment our data are consistent with an effective spin of $S = 1/2$, with strong uniaxial Ising-type anisotropy of the g tensor, that is, $g_{\parallel}^{Tb} \approx 10$, $g_{\perp}^{Tb} \approx 0$.[16–20]

The molar specific heat (C_m) data (Figure 4) can be well fitted in the range above T_c by the sum of a Debye $(T/\Theta_D)^3$ term, representing the low-temperature limiting phonon contribution, and the Schottky curve expected for a magnetic Ising $S = 1/2$ chain, with an intrachain magnetic exchange constant of $|J|/k_B = 3.6$ K and two spins of 1/2 per unit cell.

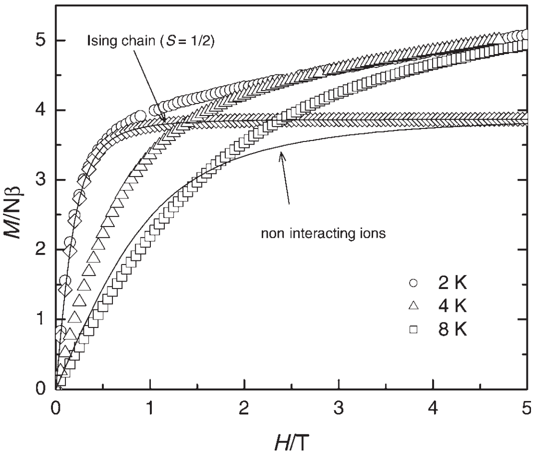

Figure 5. Field dependence of the magnetization as measured at 2, 4, and 8 K, and at 2 K with the contribution above 1 T from excited levels removed (◇). Solid lines represent the calculated curve for an Ising chain with $S=1/2$ and the Brillouin curve for noninteracting $\mathrm{Mo^{V}}$ and $\mathrm{Tb^{III}}$ ions (both at $T=2$ K).

Near and below T_c the weak interactions between the chains cause departures from the chain prediction in the form of a λ-type anomaly.[21] A slight upturn in the data below 0.5 K is attributed to the expected nuclear contribution, $C_{\rm nucl}/R = 1/3 A_{\rm hf}^2 S^2 I(I+1) T^{-2}$,[22] arising from the hyperfine (hf) interaction between the electron spin $S=1/2$ and nuclear spin $I=3/2$ (100% abundance) of the $\mathrm{Tb^{III}}$ ions. Taking the literature value for the hyperfine constant of $A_{\rm hf}/k_{\rm B}=0.28$ K, this upturn is well reproduced. The contributions from the ^{95}Mo and ^{97}Mo nuclei can be neglected here due to their low abundance (15 and 10%, respectively) and small $A_{\rm hf}$ values (5–10 mK). The value obtained for the Debye temperature ($\Theta_{\rm D} \approx 93 \pm 1$ K) is in the range typical for this type of compound. The entropy obtained from integration of the magnetic specific heat amounts to $S/k_{\rm B} \approx 1.23$, close to the value of $2\ln 2 = 1.38$ expected for two spins $S=1/2$. This confirms that the excited levels of the $\mathrm{Tb^{III}}$ ion are already depopulated below about 10 K.

For analysis of the magnetization data, we take the magnetic (Ising) interaction Hamiltonian $H_{\rm int}$ along the chains as Equation (1).

$$H_{\rm int} = -2J \sum_i S_i^{\rm Tb} S_{i+1}^{\rm Mo} - \beta H \sum_i (g^{\rm Tb} S_i^{\rm Tb} + g^{\rm Mo} S_{i+1}^{\rm Mo}) \qquad (1)$$

For the Ising model, the prediction for the specific heat in zero field is insensitive to the sign of J, but, as shown below, the magnetization data agree with a ferromagnetic intrachain interaction of the above magnitude. From the magnetization curve measured at 2 K it appears that a field of about 1 T is needed to saturate the ferromagnetic magnetization of the $\mathrm{Tb^{III}}$ and $\mathrm{Mo^{V}}$ moments in this temperature range. The subsequent slow and nearly linear increase of magnetization up to 5 T can be attributed to the contributions from the excited levels. Indeed, the slope of this high-field part gives $\chi \approx 0.24\,\mathrm{cm^3\,K\,mol^{-1}}$, about equal to the value measured with the SQUID magnetometer in low fields at $T \approx 50$ K. Extrapolating the high-field part (> 2 T) in Figure 5 to $H=0$ yields the intercept $M^{\rm total} \approx 3.9\beta$. Since we can take $M^{\rm total} = M^{\rm Mo} + M^{\rm Tb}$ and $M^{\rm Mo} = 1\beta$, we obtain $M^{\rm Tb} \approx 2.9\beta$, and thus an effective powder g value of $g_{\rm p}^{\rm Tb} \approx 5.8$ for the $\mathrm{Tb^{III}}$ ion. Indeed, since we measure on powder, we measure the spatial average of $M(\theta)$ with $g_{\rm p}^2 = (2g_\perp^2 + g_\parallel^2)/3$. For $\mathrm{Mo^{V}}$ the g value is isotropic, with $g=2$. In the spatial average of $M(\theta)$ of $\mathrm{Tb^{III}}$ we can take $g_\perp^{\rm Tb} \approx 0$ on the basis of literature values. This is indeed confirmed by our finding that $\chi_{\rm ac}$ for a powder vanishes below T_c for $T \to 0$, which indicates a very large anisotropy. Taking $g_\perp = 0$, the spatial average yields $g_\parallel^{\rm Tb} = g_{\rm p}\sqrt{3} \approx 10$ (with $g_{\rm p}^{\rm Tb} = 5.8$). The agreement with literature values of $g_\parallel^{\rm Tb}$ observed for $\mathrm{Tb^{III}}$ sites of low symmetry appears quite reasonable.[18,20] Finally, on the basis of the Hamiltonian $H_{\rm int}$, taking $g_{\rm p}^{\rm Tb} \approx 5.8$ and a ferromagnetic $J/k_{\rm B} = 3.6$ K, we calculated the powder magnetization curve expected at $T=2$ K. As seen in Figure 5, the result is in very good accord with the experiment. The Brillouin function calculated for noninteracting $\mathrm{Tb^{III}}$ and $\mathrm{Mo^{V}}$ moments at $T=2$ K is included for comparison and is obviously far from the experiment (the same applies if J is assumed to be antiferromagnetic).

As mentioned above, the transition to long-range magnetic order at $T_c = 1.0$ K is expected to arise mainly from interchain magnetic dipolar interactions. Superexchange interactions between chains via the hydrogen bonds over distances of about 8 Å will be quite weak. Magnetically, the $\mathrm{Tb^{III}}$–$\mathrm{Mo^{V}}$ chains will behave below about 2 K as ferromagnetic Ising chains formed by the $\mathrm{Tb^{III}}$–$\mathrm{Mo^{V}}$ pairs with a net magnetic moment of $\mu_{\rm pair} \approx 3.9\beta$. The dipolar interaction between two pairs on adjacent chains can be estimated as $E_{\rm dip} = \mu_{\rm pair}^2 / r_{\rm inter}^3$. With $r_{\rm inter} \approx 8$ Å as the interchain distance we obtain $E_{\rm dip}/k_{\rm b} \approx 0.04$ K, a value that may well account for the observed T_c value. To check this we can use the well-known mean-field formula $k_{\rm B} T_c^{\rm 3D} \approx \xi_{\rm 1d}(T_c) J' S^2$, from which the magnetic interchain interaction J' can be estimated from the observed 3D ordering temperature. Here, $\xi_{\rm 1d}(T) = (1/k_{\rm B}T)\text{-}\exp(J/k_{\rm B}T)$ is the magnetic correlation length along the individual Ising chains. The argument basically equates the thermal energy at the transition temperature with the interaction energy at $T=T_c$ of a reference spin with a correlated spin segment in the adjacent chain.[24] Taking $|J|/k_{\rm B} = 3.6$ K and $T_c = 1.0$ K, one obtains $|J'|/k_{\rm B} \approx 0.03$ K, reasonably close to the estimated dipolar coupling. On the basis of the available data it is not possible to conclude definitively whether the interchain dipolar ordering below T_c is ferro- or antiferromagnetic. Further studies, including field-dependent susceptibility and specific heat, are needed to further elucidate this point.

In conclusion, we have prepared and structurally characterized the first $\mathrm{Tb^{III}}$–$\mathrm{Mo^{V}}$ quasi-1D cyanido-bridged complex, which consists of ferromagnetic $\mathrm{Tb^{III}}$–$\mathrm{Mo^{V}}$ chains that become 3D magnetically ordered below $T_c = 1.0$ K. From magnetization and specific heat data, we find a ferromagnetic intrachain interaction $J/k_{\rm B} = 3.6$ K between the $\mathrm{Mo^{V}}$ and $\mathrm{Tb^{III}}$ magnetic moments. This demonstrates that the cyanido bridge between d and f ions may lead to substantial ferromagnetic superexchange coupling. A systematic study of this system varying the type of rare earth metal ion and also replacing $\mathrm{Mo^{V}}$ by $\mathrm{W^{V}}$ is in progress.

Experimental Section

1: A solution of $Tb(NO_3)_3{\cdot}5\,H_2O$ (0.25 mmol) in acetonitrile (5 mL) was added to a suspension of pyrazine-2-carboxamide (0.75 mmol) in acetonitrile (5 mL). The reaction mixture was stirred for 5 min at room temperature and then added to a solution of $(Bu_3NH)_3[Mo(CN)_8]{\cdot}4\,H_2O$ (0.25 mmol) in acetonitrile (5 mL). The resulting yellow precipitate was collected by filtration, washed with a minimum amount of acetonitrile, and dried under air. Slow evaporation of the filtrate led to the formation of microcrystalline material. Yield: 63 mg (29 %). C,H,N analysis (%) calcd: C 31.81, H 2.21, N 27.42; found: C 30.93, H 2.44, N 26.69.

Crystallographic data for **1**: $C_{23}H_{19}MoN_{17}O_5Tb$: $M_r = 868.42$, orthorhombic, space group $Pna2_1$, $a = 20.436(3)$, $b = 10.7839(10)$, $c = 14.252(2)$ Å, $V = 3140.9(7)$ Å^3, $\rho_{calcd} = 1.8365(4)$ g cm^{-3}, $Z = 4$, $\mu(Mo_{K\alpha}) = 2.696$ mm^{-1}, $T = 150$ K, 65176 reflections, 7189 of which were unique ($R_{int} = 0.0816$). The structure was solved by Patterson methods using DIRDIF and was refined on F^2 by least-squares procedures using SHELXL-97.[25] The final residuals were $R1 = 0.0301$ [4625 $F > 4\Gamma(F)$] and wR_2 0.0575 (all data). CCDC-622483 contains the supplementary crystallographic data for this paper. These data can be obtained free of charge from the Cambridge Crystallographic Data Centre via www.ccdc.cam.ac.uk/data_request/cif.

Magnetic measurements (1.8–300 K) were taken on powder samples (at 0.1 T) using a Quantum Design SQUID magnetometer. Low-temperature ac susceptibility and heat capacity data were taken in a dilution refrigerator equipped with a homemade ac susceptometer and calorimeter.

Received: April 26, 2007

Keywords: heterometallic complexes · lanthanides · magnetic properties · molybdenum · N,O ligands

---

[1] S. J. Blundell, F. L. Pratt, *J. Phys. Condens. Matter* **2004**, *16*, R771 – R828.
[2] O. Kahn, *Acc. Chem. Res.* **2000**, *33*, 647 – 657.
[3] J. S. Miller, A. J. Epstein, *Angew. Chem.* **1994**, *106*, 399 – 432; *Angew. Chem. Int. Ed. Engl.* **1994**, *33*, 385 – 415.
[4] W. R. Entley, G. S. Girolami, *Science* **1995**, *268*, 397 – 400.
[5] T. Mallah, S. Thiebaut, M. Verdaguer, P. Veillet, *Science* **1993**, *262*, 1554 – 1557.
[6] M. Ohba, H. Okawa, *Coord. Chem. Rev.* **2000**, *198*, 313 – 328.
[7] S. Tanase, J. Reedijk, *Coord. Chem. Rev.* **2006**, *250*, 2501 – 2510.
[8] M. Verdaguer, A. Bleuzen, V. Marvaud, J. Vaissermann, M. Seuleiman, C. Desplanches, A. Scuiller, C. Train, R. Garde, G. Gelly, C. Lomenech, I. Rosenman, P. Veillet, C. Cartier, F. Villain, *Coord. Chem. Rev.* **1999**, *192*, 1023 – 1047.
[9] J. M. Herrera, V. Marvaud, M. Verdaguer, J. Marrot, M. Kalisz, C. Mathoniere, *Angew. Chem.* **2004**, *116*, 5584 – 5587; *Angew. Chem. Int. Ed.* **2004**, *43*, 5468 – 5471.
[10] S. Ohkoshi, H. Tokoro, T. Hozumi, Y. Zhang, K. Hashimoto, C. Mathoniere, I. Bord, G. Rombaut, M. Verelst, C. C. D. Moulin, F. Villain, *J. Am. Chem. Soc.* **2006**, *128*, 270 – 277.
[11] B. Sieklucka, R. Podgajny, P. Przychodzen, T. Korzeniak, *Coord. Chem. Rev.* **2005**, *249*, 2203 – 2221.
[12] S. Ikeda, T. Hozumi, K. Hashimoto, S. Ohkoshi, *Dalton Trans.* **2005**, 2120 – 2123.
[13] P. Przychodzen, K. Lewinski, R. Pelka, M. Balanda, K. Tomala, B. Sieklucka, *Dalton Trans.* **2006**, 625 – 628.
[14] S. Tanase, F. Prins, J. M. M. Smits, R. de Gelder, *CrystEngComm* **2006**, *8*, 863 – 865.
[15] Z. X. Wang, X. F. Shen, J. Wang, P. Zhang, Y. Z. Li, E. N. Nfor, Y. Song, S. I. Ohkoshi, K. Hashimoto, X. Z. You, *Angew. Chem.* **2006**, *118*, 3365 – 3369; *Angew. Chem. Int. Ed.* **2006**, *45*, 3287 – 3291.
[16] R. L. Carlin, *Magnetochemistry*, Springer, Berlin, **1997**.
[17] M. Evangelisti, M. L. Kahn, J. Bartolome, L. J. de Jongh, C. Meyers, J. Leandri, Y. Leroyer, C. Mathoniere, *Phys. Rev. B* **2003**, *68*, 2534 – 2549.
[18] C. K. Loong, L. Soderholm, G. L. Goodman, M. M. Abraham, L. A. Boatner, *Phys. Rev. B* **1993**, *48*, 6124 – 6131.
[19] J. W. Orton, *Electronic Paramagnetic Resonance. An Introduction to Transition Group Ions in Crystals*, Gordon and Breach, New York, **1968**.
[20] H. Sen, D. Neogy, B. M. Wanklyn, *J. Magn. Magn. Mater.* **1988**, *73*, 221 – 228.
[21] L. J. de Jongh, A. R. Miedema, *Adv. Phys.* **2001**, *50*, 947 – 1170.
[22] A. Abragam, B. Bleaney, *Electron Paramagnetic Resonance of Transition Ions*, Clarendon, Oxford, **1970**.
[23] C. H. Anderson, E. S. Sabisky, *Phys. Rev. B* **1971**, *3*, 527 – 536.
[24] J. Villain, J. M. Loveluck, *J. Phys. Lett.* **1977**, *38*, L77 – L80.
[25] G. M. Sheldrick, *SHELXL-97, Program for Crystal Structure Solution*, University of Göttingen, Göttingen (Germany), **1997**.